Inflammation, Vol. 40, No. 6, December 2017 (© 2017)
DOI: 10.1007/s10753-017-0639-9

ORIGINAL ARTICLE

Downregulation of Paralemmin-3 Ameliorates Lipopolysaccharide-Induced Acute Lung Injury in Rats by Regulating Inflammatory Response and Inhibiting Formation of TLR4/MyD88 and TLR4/TRIF Complexes

Xuxin Chen,[1] Lu Tang,[2] Jian Feng,[3] Yi Wang,[4] Zhihai Han,[1,5] and Jiguang Meng[1,5]

Abstract— Previous studies have demonstrated paralemmin-3 (PALM3) participates in Toll-like receptor (TLR) signaling. This study investigated the effect of PALM3 knockdown on lipopolysaccharide (LPS)-induced acute lung injury (ALI) and its underlying mechanisms. We constructed a recombinant adenoviral vector containing short hairpin RNA for PALM3 to knockdown PALM3 expression. A transgene-free adenoviral vector was used as a negative control. The ALI rat model was established by LPS peritoneal injection at 48-h post-transfection. Results showed that downregulation of PALM3 improved the survival rate, attenuated lung pathological changes, alleviated pulmonary edema, lung vascular leakage and neutrophil infiltration, inhibited the production of proinflammatory cytokines and activation of nuclear factor κB and interferon β regulatory factor 3, and promoted the secretion of anti-inflammatory cytokine interleukin-10 and expression of suppressor of cytokine signaling-3 in the ALI rat model. However, PALM3 knockdown had no effect on TLR4, myeloid differentiation factor 88 (MyD88), and Toll-interleukin-1 receptor domain-containing adaptor inducing interferon β (TRIF) expression. Moreover, PALM3 knockdown reduced the interaction of TLR4 with MyD88 or TRIF induced by LPS in rat lungs. Therefore, the downregulation of PALM3 protected rats from LPS-induced ALI and its mechanisms were partially associated with the modulation of inflammatory responses and inhibition of TLR4/MyD88 and TLR4/TRIF complex formation.

Xuxin Chen, Lu Tang and Jian Feng contributed equally to this work.

[1] Department of Respiratory Medicine, Navy General Hospital of the PLA, No. 6 Fucheng Road, Beijing, 100037, China
[2] Department of Neurology, The First Hospital of Changsha, Changsha, 430100, People's Republic of China
[3] Department of Cardiology, The Affiliated Hospital of Southwest Medical University, Luzhou, 646000, China
[4] Department of Respiratory Medicine, The Sixth People's Hospital of Jinan City Affiliated to Jining Medical College, Jinan, 250200, People's Republic of China
[5] To whom correspondence should be addressed at Department of Respiratory Medicine, Navy General Hospital of the PLA, No. 6 Fucheng Road, Beijing, 100037, China. E-mails: zhihaihandoctor@163.com; mjg2016@tom.com

KEY WORDS: acute lung injury; acute respiratory distress syndrome; paralemmin-3; toll-like receptor; lipopolysaccharide; inflammation.

INTRODUCTION

Acute lung injury (ALI) and its advanced stage, acute respiratory distress syndrome (ARDS), are clinical syndromes characterized by acute hypoxemic respiratory failure, decreased pulmonary compliance, and severe imbalance of ventilation and blood flow ratio resulting from excessive pulmonary inflammation, non-cardiogenic pulmonary edema, and diffuse alveolar damage [1, 2]. Because of the lack of specific and effective treatments for ALI/ARDS, the mortality rate among these patients remains as high as 30–40% [3]. The pathogenesis of ALI/ARDS is complex, and one of the most crucial factors is an uncontrolled inflammatory response [4, 5]. Controlling the excessive inflammatory response during acute respiratory failure is an important therapeutic target for treating ALI/ARDS.

The Toll-like receptor (TLR) signaling pathway plays a key role in host defense, innate immunity, and inflammation [4, 6, 7]. Prototypic signaling in inflammation occurs through the lipopolysaccharide (LPS)-TLR4 pathway. LPS induces the dimerization of TLR4 that initiates signal transduction involving multiple adaptors, leading to the activation of inflammatory transcription factors including nuclear factor kappa beta (NF-κB) and interferon β regulatory factor 3 (IRF3), which mediates the upregulation of inflammatory cytokine gene expression leading to an inflammatory response [8, 9]. However, unchecked, excessive or inappropriate TLR signaling activation can lead to severe inflammation and immunity-related tissue damage [4, 10]. Single immunoglobulin interleukin (Ig IL)-1 receptor-related molecule (SIGIRR) is an important negative regulator of TLR signaling [10]. Through the negative regulation of TLR signaling, SIGIRR can depress the inflammatory response to LPS, block the transduction cascade, inhibit NF-κB activation, decrease the production of inflammatory mediators, and ultimately attenuate organ injury [11]. Trapping key components of the TLR signaling pathway is the mechanism by which SIGIRR inhibits TLR signaling transduction [4, 5]. The Toll-interleukin-1 receptor (TIR)-domain of SIGIRR is necessary for SIGIRR to interact with TIR-domain containing adaptors [12].

Paralemmin (PALM)-3 belongs to the PALM protein family and was first described in *Xenopus laevis* as Xlgv7/Xlcaax-1 by Cornish et al. [13]. In our previous study, we used the C-terminal part of SIGIRR containing the TIR domain as bait to screen SIGIRR-binding proteins in a human lung cDNA library and found that PALM-3 is a novel interactive partner of SIGIRR [12]. We also showed that silencing PALM3 expression inhibited the release of inflammatory cytokines induced by LPS *in vitro* [12]. Moreover, previous research demonstrated that the downregulation of PALM3 was protective against LPS-induced ALI in mice [14]. Although the downregulation of PALM3 has been shown to benefit LPS-induced ALI in mice, the explicit underlying mechanisms against ALI, including whether the downregulation of PALM3 has a protective effect against LPS-induced ALI in other animal models, a negative effect on the expression of adaptors in the LPS-TLR4 pathway, blocks LPS-TLR4 signal transduction, and regulates the inflammatory transcription factors NF-κB and IRF3, remain unclear. Indeed, species diversity usually leads to different research results, even under the same experimental conditions. For example, comprehensive physiologic studies of lung injury are better in rats than in mice [15]. Therefore, the present study investigated the effect of the downregulated expression of PALM3 on LPS-induced ALI using a rat model.

To elucidate the potential mechanisms involved, the production of pro- and anti-inflammatory cytokines in bronchoalveolar lavage fluid (BALF) and serum, and the expression of TLR4, myeloid differentiation factor 88 (MyD88), TIR domain-containing adaptor inducing interferon β (TRIF), and NF-κB and IRF3 activities in the lungs were examined. Additionally, the interaction of TLR4 with MyD88 or TRIF in rat lung was also detected by co-immunoprecipitation.

MATERIALS AND METHODS

Cell Culture

Cells in the exponential growth phase were used in the experiments described below. HEK 293 cells (Microbix, Toronto, Canada) were grown in Dulbecco's modified Eagle's medium (Gibco/BRL, Grand Island, NY), supplemented with 10% fetal bovine serum (Gibco/BRL), 100 U/mL penicillin, 100 U/mL streptomycin, and 2 mmol/L L-glutamine (Gibco/BRL) at 37 °C in a humidified chamber with 5% CO2. HEK 293 cells were seeded in 75 m^2 flasks or 6-well plates (5×10^5/well) prior to transfection.

Generation of Adenoviral Vectors

In accordance with the principles of RNA interference sequence design, the sequence 5′-AGATCTTGATGGAG GGTTT-3′ was chosen as the target sequence. The primers for this target sequence were 5′-CCGGGGAGATCTTG ATGGAGGGTTTCTCGAGAAACCCTCCATCA AGATCTCCTTTTTG-3′ (sense) and 5′-AATT CAAAAAGGAGATCTTGATGGAGGGTTTC TCGAGAAACCCTCCATCAAGATCTCC-3′ (antisense) (GeneChem Co. Ltd., Shanghai, China). The short hairpin oligonucleotide and complementary strand targeting the consensus sequences of PALM3 were designed and inserted into the shuttle plasmid pGV120 (GeneChem) to generate the plasmid pGV120-PALM3-shRNA. The pGV120-PALM3-shRNA plasmid was identified by PCR and DNA sequencing. Recombinant viruses were generated using 293 packaging cells cotransfected with the shuttle plasmid and the framing plasmid (pBHGlox) *via* the AdMax™ system (Microbix). Viral stocks were purified using CsCl gradients. The recombinant virus was named Ad.PALM3-shRNA. A control vector containing no transgene (Ad.V) was constructed using the same method. Titers of the recombinant adenoviruses were determined by means of 50% tissue culture infectious dose, and for Ad.PALM3-shRNA and Ad.V, this was 3×10^{10} plaque-forming units (PFU)/mL and 6×10^{10} PFU/mL, respectively.

Establishment of ALI Rat Model and Experimental Design

Adult Wistar rats (8 weeks old) were purchased from the Laboratory Animal Center of the Academy of Military Medical Sciences (Certificate number SCXK-Army-2012-0004, Beijing, China). All rats used in this research were raised and used in accordance with the ARRIVE (Animal Research: Reporting of *In Vivo* Experiments) Guidelines on the Use of Laboratory Animals [16] and the care and housing of rats were approved by the Animal Care and Use Committee of Navy General Hospital (Approval number: SCXK-Army-2012-0012). Animals were housed in specific pathogen-free conditions at a regular temperature (22 ± 2 °C) and humidity (50 ± 10 °C) with a standard diet and clean water provided *ad libitum*. After acclimatization for 1 week in the animal housing facility, rats were anesthetized by ether (Fuyu Chemical Co., Ltd., Tianjin, China) inhalation as follows: cotton wool containing ether was placed in an animal anesthesia bottle and the rats were placed into this bottle for 5 min. After the rats were lightly anesthetized, they were removed and inoculated intranasally with a total of 3×10^8 PFU (in 100 μL) of Ad.PALM3-shRNA (Ad.PALM3-shRNA group) or Ad.V (Ad.V group) using a 1-mL blunt head syringe as previously described [4, 17]. Forty-eight hours later, LPS (*Escherichia coli* 0127: B8, Sigma-Aldrich, St. Louis, MO, USA) at 15 mg/kg (dissolved in saline) was injected into the peritoneal cavity of conscious rats to establish the ALI rat model. Rats were sacrificed with a supraphysiological dose of pentobarbital sodium (100 mg/kg) at 0, 3, 6, 12, 24, or 48 h after LPS challenge (n = 6 per time point in each group). After each rat was sacrificed, an 18-gauge sterile catheter (Carelife Co. Ltd., Shanghai, China) was inserted into the left bronchus to collect BALF as previously described [18]. The right lungs were rapidly removed from all rats and washed in RNase-free ice-cold saline. The upper lobe of the right lung was frozen in 1 mL TRIzol Reagent (Invitrogen, Shanghai, China) and stored in liquid nitrogen for RNA extraction. The middle lobe of the right lung was frozen in 1 mL cell lysis buffer (Beyotime Chemical Co., Jiangsu, China) and stored in liquid nitrogen for protein isolation and tissue homogenization. The lower lobe of the right lung was immediately fixed with 4% paraformaldehyde phosphate buffer solution (Bosterbio, Wuhan, China) for histological evaluation. Blood samples were obtained from the right side of the heart (1–2 mL per rat), allowed to clot for 0.5 h on ice, and then centrifuged at 3000×g for 30 min (4 °C). The sera were stored in small aliquots at − 70 °C until the cytokine levels were measured.

Determination of PALM3 mRNA Expression

Total RNA was extracted from the lung tissue using TRIzol Reagent (Invitrogen) according to the manufacturer's instructions. The RNA was further purified by an RNA Cleanup Kit (CWBIO Co., Beijing, China). Reverse transcription (RT) of the lung samples was performed using the Takara Primescript RT Reagent Kit (TaKaRa, Dalian, China). Then, quantitative real-time polymerase chain reaction (qRT-PCR) was performed using iTaq Universal SYBR Green Supermix (TaKaRa) according to the manufacturer's instructions. The primers for rat PALM3 were 5′-GAGGCAGGGATCTTGATGTC-3′ (sense) and 5′-GCCCAACACCCTCAAGACTA-3′ (antisense) (TaKaRa). The primers for rat β-actin were 5′-GGAG ATTACTGCCCTGGCTCCTA-3′ (sense) and 5′-GACT CATCGTACTCCTGCTTGCTG-3′ (antisense) (TaKaRa). β-actin was selected as an internal standard. The PCR parameters were set as 95 °C for 30 s, followed by 35 cycles of 95 °C for 5 s and 60 °C for 30 s. All reactions were

performed in triplicate, and reports were generated by Rotor-Gene Real-Time Analysis Software 6.0 (Corbett Research, Australia). The relative expression of the target genes (PALM3 and β-actin) was calculated by the $2^{-\Delta\Delta Ct}$ method.

Western Blot Analysis of PALM3

Protein was extracted from the lung tissue as previously described [4, 5]. Protein concentrations were measured by the bicinchoninic acid (BCA) method (Sigma-Aldrich) at 562 nm with a μQuant microplate spectrophotometer (BioTek Inc., Winooski, VT, USA). Protein samples were analyzed by western blotting. Equal amounts of protein were separated by 15% sodium dodecyl sulfate (SDS)/polyacrylamide gel electrophoresis (PAGE) and transferred onto a polyvinylidene fluoride filter membrane in a semidry blotting apparatus (Bio-Rad Co. Ltd., Shanghai, China). To reduce non-specific binding, the membrane was blocked in a 5% (*w/v*) non-fat milk (Beyotime) solution in Tris-buffered saline-Tween (TBST: 140 mM NaCl, 10 mM Tris/HCl, pH 7.4 and 0.05% Tween 20) (Beyotime) at 37 °C for 2 h. The membranes were then incubated with anti-PALM-3 (cat. no. sc-248,213; polyclonal goat anti-rat; Santa Cruz) (1:500 in TBST) and anti-β-actin antibodies (cat. no. AF0003; monoclonal mouse anti-rat; Beyotime) (1:500 in TBST) overnight at 4 °C. After extensive washing with TBST, the membranes were incubated with horseradish peroxidase (HRP)-conjugated secondary antibody (1:2000 in TBST) (Beijing Golden Bridge Biotech, Beijing, China) at room temperature for 2 h. The blots were washed twice in TBST buffer and the signals were detected by enhanced chemiluminescence following the manufacturer's instructions (Beyotime). The membrane was photographed using the Gel Documentation and Analysis System (GBOX-HR, Syngene, USA), and band intensities were measured with Adobe Photoshop version 7.0.1 software (Adobe Systems, USA) and normalized to the expression of β-actin for quantitative analysis.

Rat Survival Rate

A second cohort of rats (n = 30) was used to evaluate the effect of Ad.PALM3-shRNA on the outcome of LPS-induced ALI. Rats were divided into two groups (n = 15 rats per group) and given the same treatment as previously described. Seven-day survival rates were recorded and analyzed.

Histological Evaluation

Lung tissues were treated with a 4% paraformaldehyde-phosphate buffer solution (Bosterbio) (pH = 7.4) overnight at 4 °C, dehydrated, embedded, and sectioned to 5.0-μm thickness. Tissue slides were then stained with hematoxylin and eosin (HE) (Bosterbio) and analyzed under identical light microscope conditions (Olympus Co., Ltd., Tokyo, Japan). Lung injury was scored by a blinded observer according to the following three criteria: (1) alveolar and interstitial edema, (2) alveolar hemorrhage, and (3) infiltration or aggregation of neutrophils. Each criterion was graded according to a four-point scale: 0 = normal, 1 = mild change, 2 = moderate change, and 3 = severe change. The scores for criteria 1 to 3 were summed to represent the lung damage score (total score: 0–9) [4, 5].

Collection of BALF and Analysis of BALF Total Protein

The left lungs were lavaged five times with PBS (1 ml each time) and approximately 80% of the instilled volume was retrieved [18, 19]. BALFs were then centrifuged at 1000×*g* for 5 min (4 °C), and the clear supernatant was transferred to sterile Eppendorf tubes and stored at − 70 °C for the analysis of total protein concentration [18, 20] by the BCA method (Sigma-Aldrich).

Lung Wet/Dry Ratios

Adult Wistar rats (n = 6 per group) were treated as described in the "Materials and Methods" section "Establishment of ALI Rat Model and Experimental Design." At 24 h after LPS challenge, the right lungs were harvested and stored in liquid nitrogen for the analysis of NF-κB phospho-p65, phospho-IRF3, TLR4, MyD88, TRIF, suppressor of cytokine signaling 3 (SOCS3) protein levels and coimmunoprecipitation assay, and the left lungs were harvested for the analysis of lung wet/dry weight ratio. The lung tissues were weighed immediately then subjected to desiccation in a 70 °C oven until a stable dry weight was achieved after 72 h. The scales and oven were purchased from Whaisp Scientific Instrument Co., Ltd. (Wuhan, China). The wet/dry weight ratio was calculated by dividing the wet weight with the dry weight to quantify the magnitude of pulmonary edema [19].

Measurement of BALF Neutrophils

BALF was prepared as described above, and BALF pellets were resuspended in cold PBS (4 °C). BALF (100 μL) was mounted on a glass slide by centrifugation and the glass slide was stained with HE (Bosterbio). For analysis of the neutrophil cell count, we counted 200 cells per slide in randomly selected high-powered fields (× 1000) under identical light microscope conditions (Olympus). BALF neutrophil cell counts were expressed as cell count/mL of BALF [20].

Determination of Lung Myeloperoxidase Activity

To measure tissue myeloperoxidase (MPO) activity, frozen lungs were thawed and MPO was extracted following the homogenization and sonication procedure described previously [4]. MPO activity in the supernatant was measured at an absorbance of 460 nm, and changes in MPO activity were determined following the decomposition of H_2O_2 in the presence of o-dianisidine. The specific activity of MPO in the lung was expressed as U/g of the wet lung tissue.

Detection of Cytokine Levels

Serum and BALF were prepared as described above. Levels of tumor necrosis factor-α (TNF-α), interleukin-1β (IL-1β), IL-10 (R&D Systems, Inc., Minneapolis, MN), and interferon β (IFN-β) (Cusabio, Wuhan, China) in BALF and serum were measured by commercially available enzyme-linked immunosorbent assay (ELISA) kits for rat, following the manufacturer's instructions. In brief, diluted standards or samples were added to 96-well plates precoated with affinity purified polyclonal antibodies specific for TNF-α, IL-1β, IL-10, and IFN-β, respectively. Enzyme-linked polyclonal antibodies were then added to the wells prior to incubation at 37 °C for 60 min, followed by five final washes. The intensities detected at 450 nm were measured after the addition of substrate solutions for 15 min. Each sample was assayed in triplicate. Levels of TNF-α, IL-1β, IL-10, and IFN-β were calculated according to standard curves.

ELISA for the Detection of NF-κB Activity

Nuclear extracts were prepared using the NE-PER Nuclear-Cytoplasmic Extraction Reagents kit (Thermo Fisher Scientific, USA) according to the manufacturer's protocol. The extracts were stored at − 70 °C, and the protein concentration of the nuclear extracts was quantified by the BCA method (Sigma-Aldrich). NF-κB p65 DNA binding activity was assessed on isolated nuclear extracts by ELISA using the TransAM™ NF-κB Transcription Factor Assay kit according to the manufacturer's protocol (Active Motif, Carlsbad, CA) [4]. Each sample was assayed in triplicate. Equal amounts of Raji nuclear extract were used as positive controls.

Western Blot Analysis of NF-κB Phosho-p65, Phospho-IRF3, TLR4, MyD88, TRIF, and SOCS3

Lung tissues samples were obtained as described in the "Materials and Methods" section "Lung Wet/Dry Ratios." The nuclear extract and total protein were prepared, and the procedure of western blot analysis was performed as described above. Expressions of NF-κB phospho-p65 and phospho-IRF3 in the nuclear extracts were analyzed by immunoblotting with phospho-specific anti-NF-κB p65 (cat. no. AN371; monoclonal rabbit anti-rat; Beyotime) (1:500 in TBST) antibody or phospho-specific anti-IRF3 (cat. no. ab138449; polyclonal rabbit anti-rat; Abcam, Cambridge, UK) (1:500 in TBST) antibody, and histone H3 (cat. no. sc-374,669; monoclonal mouse anti-rat; Santa Cruz) (1:1000 in TBST) was used as a lysate control. Expressions of TLR4, MyD88, TRIF, and SOCS3 in total protein were analyzed by immunoblotting with anti-TLR4 (cat. no. sc-293,072; monoclonal mouse anti-rat; Santa Cruz) (1:500 in TBST), anti-MyD88 (cat. no. 4283; monoclonal rabbit anti-rat; Cell Signaling Technology) (1:1000 in TBST), rabbit polyclonal anti-TRIF (cat. no. ab13810; polyclonal rabbit anti-rat; Abcam, Cambridge, UK) (1:500 in TBST), or anti-SOCS3 (cat. no. sc-73,045; monoclonal mouse anti-rat; Santa Cruz) (1:200 in TBST). β-actin (Beyotime) (1:1000 in TBST) was used as a lysate control. Corresponding HRP-conjugated secondary antibodies (Beijing Golden Bridge) were used to display the protein signal.

Coimmunoprecipitation Assay

To examine endogenous protein–protein interactions, coimmunoprecipitation assays were performed. Lung tissue samples were obtained as described in the "Materials and Methods" section "Lung Wet/Dry Ratios." Protein was extracted from the lung tissue as previously described [21]. The rat lung tissue was homogenized and lysed in TNE buffer (10 mM Tris, pH 8.0, 150 mM NaCl, 1 mM EDTA, 1% NP-40, 10% glycerol with protease inhibitor cocktail [Sigma-Aldrich]) (8 ml of TNE/g lung lysate) and clarified by centrifugation at 14,000×*g* for 15 min at 4 °C. After centrifugation, proteins were quantified using the BCA method (Sigma-Aldrich). Approximately 10 mg

samples of rat lung lysates were incubated with a primary rat-specific anti-TLR4 (25) antibody (1:100 in TBST) (cat. no. sc-293,072; monoclonal mouse anti-rat; Santa Cruz), and the same amount of lysate was incubated with normal rat IgG (Santa Cruz) as a negative control at 4 °C for 2 h and then with 20 μl of protein A/G-agarose (Beyotime) at 4 °C with rocking overnight. The pellets obtained after centrifugation were washed five times with washing buffer (50 mM Tris (pH 7.5), 7 mM $MgCl_2$, 2 mM EDTA, and 1 mM PMSF). The pellets were resolved by SDS-PAGE and boiled for 10 min. After centrifugation, the supernatants were obtained as immunoprecipitates for western blotting analysis by using anti-TLR4 antibody (Santa Cruz), anti-MyD88 antibody (Cell Signaling Technology), or anti-TRIF antibody (Abcam).

Statistical Analysis

Data are expressed as the means ± standard error of the mean (SEM). Statistical significance was estimated by one-way analysis of variance (ANOVA) followed by the Student-Newman-Keuls test. Kaplan-Meier curves and the log-rank test were used to assess survival data. Statistical significance was determined for *P* values less than 0.05.

RESULTS

PALM3 Gene and Protein Expression in Lung Tissues

Lung tissues were obtained at 0, 3, 6, 12, 24, and 48 h after LPS injection to detect PALM3 expression using quantitative real-time polymerase chain reaction (qRT-PCR) and western blot analysis. In the Ad.V group, PALM3 gene and protein expression in the lung tissues increased significantly, peaking at 24 h after LPS challenge ($P < 0.05$ *vs.* 0-h time point; $P > 0.05$ 24-h *vs* 48-h time point) (Fig. 1), indicating that LPS enhanced PALM3 expression in a time-dependent manner. This result was consistent with our previous report *in vitro* [12]. The administration of Ad.V did not influence PALM3 expression before LPS stimulation ($P > 0.05$ *vs.* normal rats) (Fig. 1). Compared with the Ad.V group and normal rats, PALM3 mRNA and protein expression in the Ad.PALM3-shRNA group were significantly decreased, although increases were noted after LPS stimulation at 6 h ($P < 0.05$ *vs.* Ad.V group at each time point) (Fig. 1). Moreover, the PALM3 expression levels in the Ad. PALM3 group decreased by about 50% compared with those in the Ad.V group at each time point.

Downregulation of PALM3 Improves the 7-Day Survival Rate of ALI Rats

To determine the effect of the downregulation of PALM3 expression on the outcome of LPS-induced ALI, survival rates of the Ad.V and Ad.PALM3-shRNA groups were compared using the log-rank test. Compared with the Ad.V group, the survival rate of the Ad.PALM3-shRNA group was significantly increased. Rats receiving the Ad.PALM3-shRNA and control adenoviral vectors had an overall survival rate of 67 and 33%, respectively, over 7 days ($P < 0.05$) (Fig. 2).

Downregulation of PALM3 Improves Lung Histological Changes

Histopathological staining showed that lung sections from the Ad.V group displayed typical histological features of ALI after LPS challenge, including the infiltration

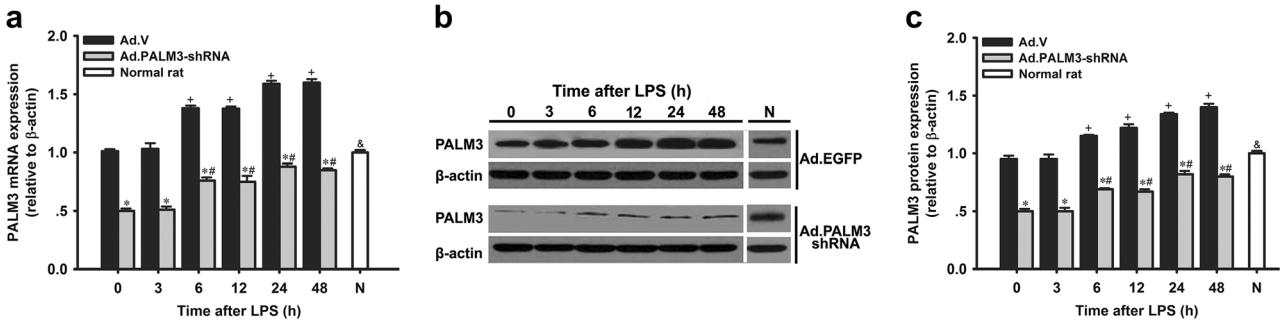

Fig. 1. PALM3 expression in lungs at different time points after LPS injection. **a** PALM3 mRNA levels in lungs at 0, 3, 6, 12, 24, and 48 h after LPS injection measured by qRT-PCR. **b** Representative image of western blot analysis for PALM3 protein levels. **c** Western blot analysis of PALM3 protein levels in lungs at 0, 3, 6, 12, 24, and 48 h after LPS injection. Data are expressed as means ± SEM ($n = 6$). *$P < 0.05$ *vs.* Ad.V group at each time point, $^{\&}P < 0.05$ *vs.* Ad.PALM3-shRNA group at each time point, #$P < 0.05$ *vs.* Ad.PALM3-shRNA group at 0 h time point, and +$P < 0.05$ *vs.* Ad.V group at 0 h time point. "*N*" indicates normal and untreated rats.

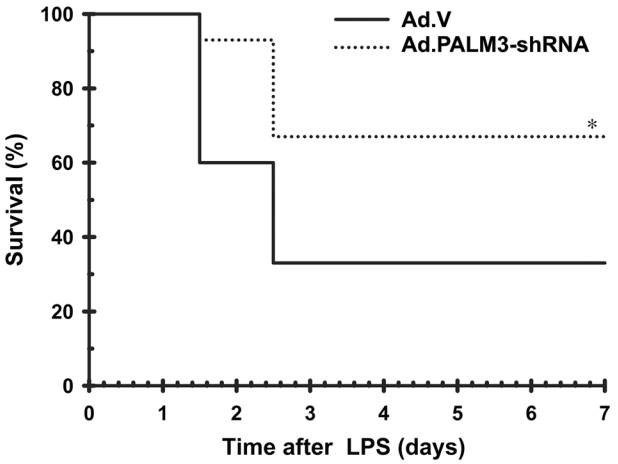

Fig. 2. Downregulation of PALM3 improves the survival rate of LPS-challenged rats. Rats were pretreated with Ad.PALM3-shRNA or Ad.V (n = 15 per group) 48 h before LPS injection. Survival was recorded for 7 days and survival curves were compared by log-rank test. Values are expressed as survival percentage. *$P < 0.05$ *vs.* Ad.V group.

of numerous neutrophils, alveolar congestion and hemorrhage, and marked swelling of the alveolar walls. Moreover, the magnitude of lung injury was increased over time (Fig. 3a (a–e)). Ad.PALM3-shRNA pretreatment improved these LPS-induced histological changes of lung tissue compared with the Ad.V group (Fig. 3a (a–j)). In addition, we used a pathological scoring system to quantify the severity of lung tissue damage in both groups. As shown in Fig. 3b, the lung injury scores of both groups were very low before LPS stimulation, demonstrating that the adenovirus vector had no impact on lung injury (Fig. 4b). Furthermore, the lung injury scores in the Ad.PALM3-shRNA group were significantly decreased at each time point after LPS challenge compared with those in the Ad.V group ($P < 0.05$ *vs.* Ad.V group at each time point) (Fig. 3b).

Downregulation of PALM3 Decreases Lung Vascular Permeability

Because protein concentrations in the BALF and lung water content are usually used to quantify the increase of vascular permeability in ALI, we measured total protein levels in BALF and lung wet/dry ratios in both groups. The concentration of total protein in the BALF of both groups increased after LPS-stimulation ($P < 0.05$ *vs.* 0-h time point) (Fig. 4a). However, total protein levels in the BALF of the Ad.PALM3-shRNA group were significantly lower than those in the Ad.V group after LPS stimulation ($P < 0.05$ *vs.* Ad.V group at each time point) (Fig. 4a). This result also demonstrated that the total protein level in the BALF of both groups reached a peak at 24 h after LPS stimulation (Fig. 4a), indicating that lung vascular leakage was most severe at the 24-h time point. Consequently, the lung wet/dry ratios at this time point were measured to confirm changes of lung vascular permeability. We found that LPS led to increased lung wet/dry ratios in both Ad.V and Ad.PALM3-shRNA groups ($P < 0.05$ *vs.* normal rats) (Fig. 4b), and Ad.PALM3-shRNA pretreatment markedly attenuated LPS-induced pulmonary edema ($P < 0.05$ *vs.* LPS-treated and LPS + Ad.V-treated rats) (Fig. 4b).

Downregulation of PALM3 Reduces Neutrophil Counts in BALF and MPO Activities in Lung

BALF neutrophil counts commonly indicate the severity of inflammation in ALI. As shown in Fig. 5a, the BALF neutrophil count was significantly increased in the Ad.V group after LPS injection ($P < 0.05$ *vs.* 0-h time point) (Fig. 5a). However, in the Ad.PALM3-shRNA group, the BALF neutrophil count was significantly decreased at each time point after LPS exposure ($P < 0.05$ *vs.* group Ad.V at each time point) (Fig. 5a). Myeloperoxidase (MPO) activity is an index of neutrophil sequestration. Thus, the MPO activity in lung tissue was detected to determine the extent of neutrophil infiltration. MPO activity was normalized by the weight of wet lung tissue. In unstimulated rats, MPO levels in the lung tissues were very low (0.48 ± 0.07 U/g wet lung tissue in the Ad.V group and 0.48 ± 0.08 U/g wet lung tissue in the Ad.PALM3-shRNA group) (Fig. 5b). MPO activities in lung tissues increased sharply after LPS injection in both groups ($P < 0.05$ *vs.* 0-h time point) (Fig. 5b). Nevertheless, increases of MPO activity in the lung were significantly decreased in the Ad.PALM3-shRNA group at each time point after LPS exposure compared with that in the Ad.V group ($P < 0.05$ *vs.* group Ad.V at each time point) (Fig. 5b).

Downregulation of PALM3 Reduces IL-1β and IFN-β Levels in the BALF and Serum

Increased levels of proinflammatory cytokines are an indication of local pulmonary injury/systemic inflammation in ALI, as reported previously [4, 20, 22]. Thus, we evaluated levels of the proinflammatory cytokines TNF-α, IL-1β, and IFN-β in the BALF and serum. When Ad.PALM3-shRNA and Ad.V were administered without LPS treatment, there were no significant differences in cytokine levels in BALF and serum between the two groups ($P > 0.05$) (Fig. 6). After LPS stimulation, the levels of TNF-α (Fig. 6a, b), IL-1β (Fig. 6c, d), and IFN-β (Fig. 6e, f) in

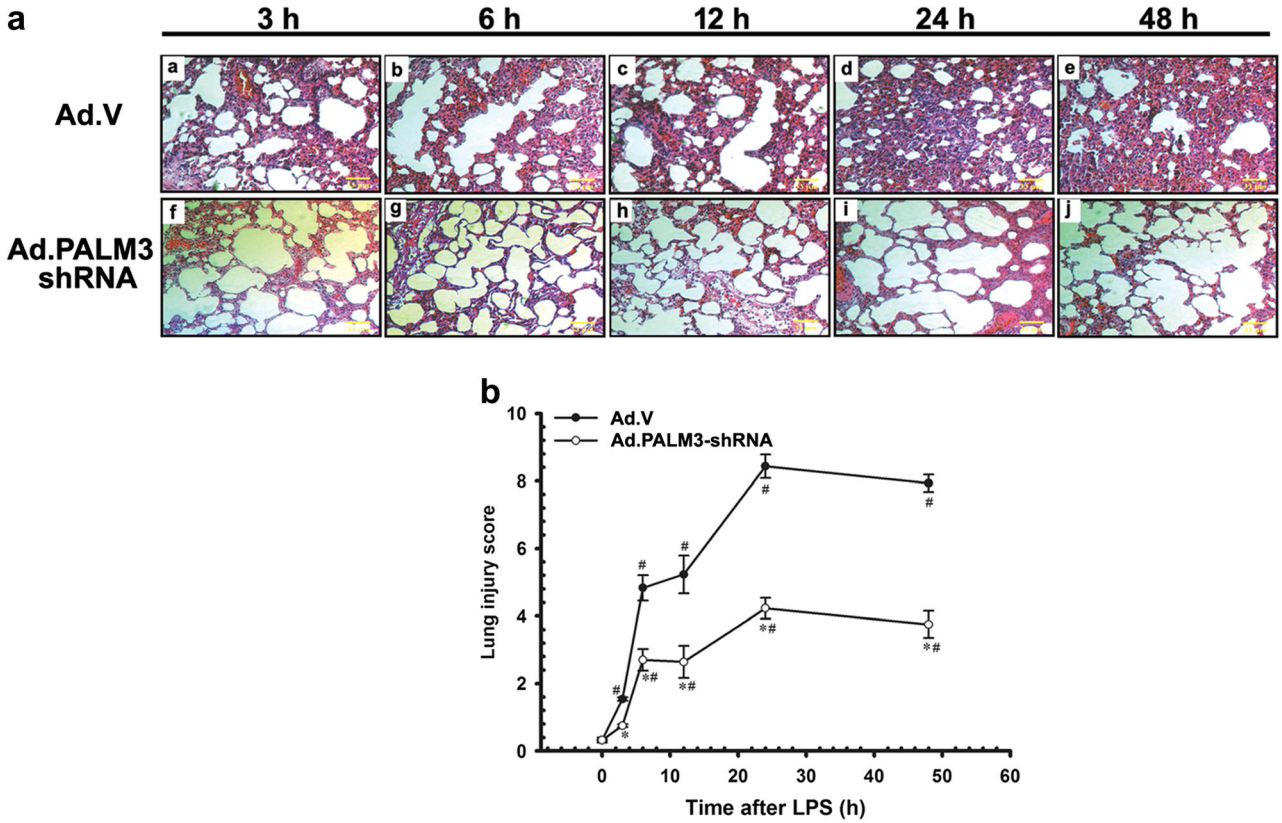

Fig. 3. Downregulation of PALM3 alleviates lung histopathological injury in LPS-challenged rats. **a** Representative hematoxylin-eosin (HE) stained histological lung sections at different time points after LPS injection. At least three images were taken per field of view per sample. (original magnification × 200). **b** Lung damage score at 0, 3, 6, 12, 24, and 48 h after LPS challenge. Data are expressed as means ± SEM ($n = 6$). *$P < 0.05$ *vs.* Ad.V group at each time point and #$P < 0.05$ *vs.* 0 h time point.

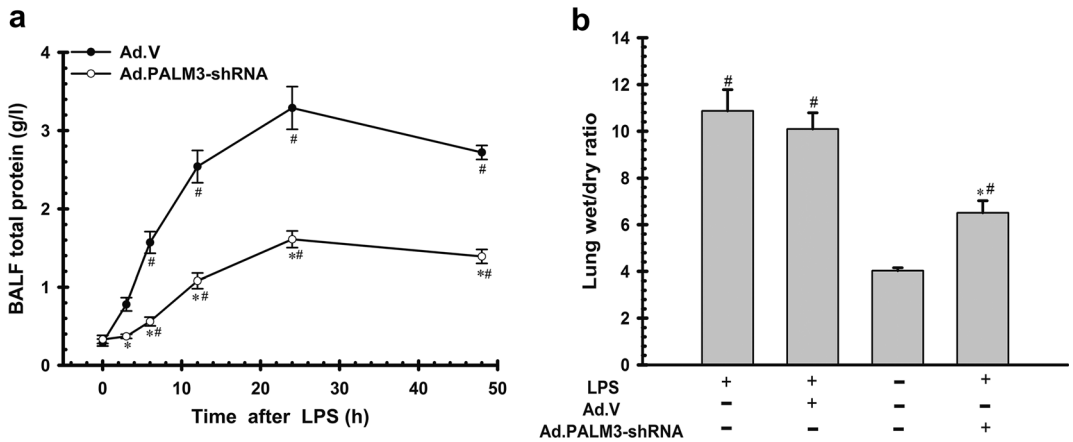

Fig. 4. Downregulation of PALM3 decreases lung vascular permeability. **a** Downregulation of PALM3 significantly decreased total protein in BALF. Data are expressed as means ± SEM ($n = 6$). *$P < 0.05$ *vs.* Ad.V group at each time point and #$P < 0.05$ *vs.* 0 h time point. **b** Downregulation of PALM3 significantly decreased lung wet/dry ratios at 24 h after LPS injection. Normal and ALI rats were used as control groups. Data are expressed as means ± SEM ($n = 6$). *$P < 0.05$ *vs.* LPS-treated and LPS + Ad.V-treated rats and #$P < 0.05$ *vs.* normal and untreated rats.

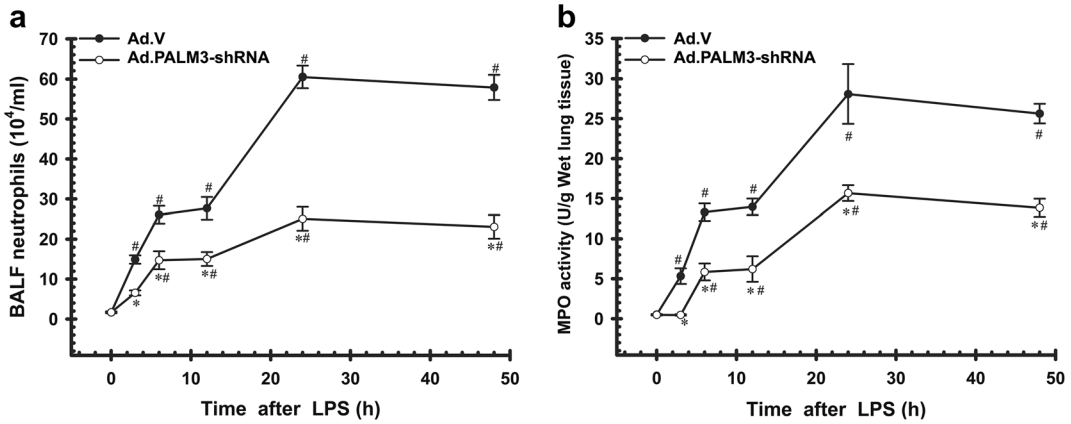

Fig. 5. Downregulation of PALM3 decreased neutrophil counts in BALF and MPO activity in lung. BALF and lung tissues were collected and neutrophil counts in the BALF (**a**) and MPO activity in the lung (**b**) were analyzed. Data are expressed as means ± SEM ($n = 6$). *$P < 0.05$ *vs.* Ad.V group at each time point and #$P < 0.05$ *vs.* 0 h time point.

BALF and serum were significantly increased in the Ad.V group. In contrast, Ad.PALM3-shRNA pretreatment reduced the elevated levels of TNF-α (Fig. 6a, b), IL-1β (Fig. 6c, d), and IFN-β (Fig. 6e, f) in BALF and serum ($P < 0.05$ *vs.* Ad.V group at each time point) (Fig. 6).

Downregulation of PALM3 Enhances IL-10 Secretion and SOCS3 Expression

IL-10 is an anti-inflammatory cytokine with negative immune regulatory effects in the TLR4 inflammatory signal transduction pathway [23]. Thus, we evaluated the levels of anti-inflammatory cytokine IL-10 in the BALF and serum. LPS exposure increased the levels of IL-10 in the BALF (Fig. 7a) and serum (Fig. 7b). In the Ad.PALM3-shRNA-treated group, the LPS-induced increase of IL-10 was further enhanced compared with the Ad.V-treated group ($P < 0.05$ *vs.* Ad.V group at each time point) (Fig. 7). SOCS3 is an important negative regulator of inflammation and plays a protective role in LPS-induced lung inflammatory responses [24, 25]. Previous studies have shown that IL-10 induced SOCS3 expression [23, 25]. Thus, we evaluated the protein levels of SOCS3 in lung tissues using western blot analysis. The results showed that LPS induced the expression of SOCS3 in all LPS-treated rats ($P < 0.05$ *vs.* normal rat) (Fig. 7c). However, Ad.rPALM3 pretreatment further increased the elevated SOCS3 protein levels in lung tissues ($P < 0.05$ *vs.* LPS-treated and LPS + AdV-treated rats) (Fig. 7c).

Downregulation of PALM3 Suppresses NF-κB and IRF3 Activities in Lung Tissue

NF-κB is considered a key transcription factor in LPS-TLR4 signaling that mediates LPS-induced ALI [26]. Thus, the NF-κB-DNA-binding activity and NF-κB phospho-p65 protein level in rat lungs was determined as described above. The ELISA result showed that all LPS-injected rats exhibited an increase in NF-κB-DNA-binding in comparison with LPS-free rats ($P < 0.05$ *vs.* 0-h time point) (Fig. 8a). Ad.PALM3-shRNA pretreatment significantly attenuated the LPS-induced increase in NF-κB activation compared with the Ad.V group ($P < 0.05$ *vs.* Ad.V group at each time point) (Fig. 8a). ELISA demonstrated that the activity of NF-κB reached a peak at 24 h after LPS stimulation (Fig. 8a). Therefore, we also examined the NF-κB phospho-p65 protein level in nuclear extracts at this time point using western blot analysis to confirm the inhibitory action of Ad.PALM3-shRNA on LPS-induced NF-κB activation. As shown in Fig. 8b, at 24 h after LPS stimulation, the NF-κB and phospho-p65 protein levels in the Ad.PALM3-shRNA group were reduced by about 30% compared with those in LPS-treated and LPS + Ad.V-treated rats ($P < 0.05$) (Fig. 8b). IRF3 is also an important transcription factor in cells and activates the IFN-β gene to regulate the release of

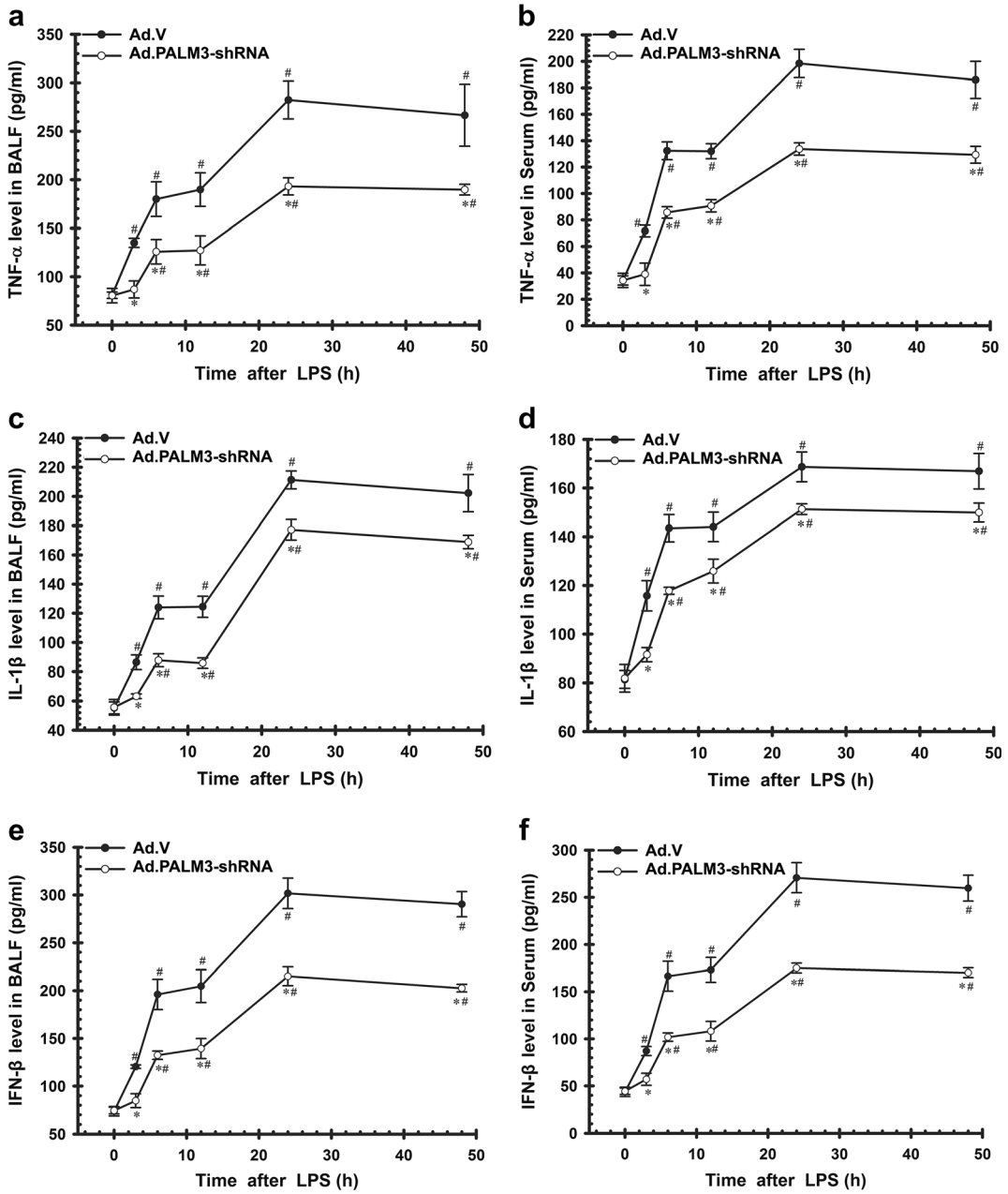

Fig. 6. Downregulation of PALM3 decreases LPS-induced proinflammatory cytokine production in BALF and serum. BALF and serum were collected and TNF-α (**a**, **b**), IL-1β (**c**, **d**), and IFN-β (**e**, **f**) levels were measured. Data are expressed as means ± SEM ($n = 6$). *$P < 0.05$ *vs.* Ad.V group at each time point and #$P < 0.05$ *vs.* 0 h time point.

proinflammatory cytokines induced by LPS [23]. We therefore examined the phospho-IRF3 protein levels in nuclear extracts using western blot analysis to detect the influence of PALM3 on LPS-induced IRF3 activation. At 24 h after LPS stimulation, phospho-IRF3 protein levels were significantly increased in all rats. However, Ad.rPALM3 pretreatment reduced the elevated phospho-IRF3 protein levels ($P < 0.05$ *vs.* LPS-treated and LPS + Ad.V-treated rats) (Fig. 8c).

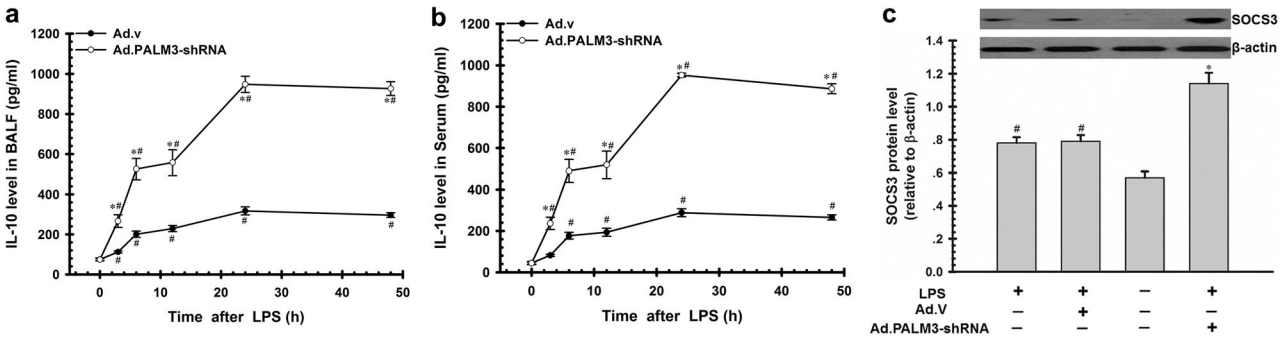

Fig. 7. Downregulation of PALM3 increases LPS-induced anti-inflammatory cytokine IL-10 secretion in BALF and serum and SOCS3 expression in lungs. Rats were instilled with 100 μL of Ad.PALM3-shRNA or Ad.V intranasally. At 48 h, lung injury was induced by a peritoneal injection of LPS (15 mg/kg). BALF and serum were collected to analyze the level of IL-10 in the BALF (**a**) and serum (**b**). Data are expressed as means ± SEM ($n = 6$). *$P < 0.05$ *vs.* Ad.V group at each time point and #$P < 0.05$ *vs.* 0 h time point. **c** Detection of SOCS3 protein levels in lung tissues at 24 h after LPS-stimulation by western blot. Upper panel of **c** is a representative photograph. Normal and ALI rats were used as controls. Data are expressed as means ± SEM ($n = 6$). *$P < 0.05$ *vs.* LPS-treated rats and LPS + Ad.V-treated rats and #$P < 0.05$ *vs.* normal rats.

Effects of Downregulation of PALM3 on LPS-Induced TLR4, MyD88, and TRIF Protein Expression

TLR4, MyD88, and TRIF are important adaptors in the TLR4 signaling pathway [27]. Thus, we examined TLR4, MyD88, and TRIF expression levels in lung tissues using western blot analysis to detect the influence of PALM3 on their expression in the ALI rat model. As shown in Fig. 9, LPS significantly induced the expression of TLR4, MyD88, and TRIF in lung tissues ($P < 0.05$ *vs.* normal rats). However, PALM3 shRNA and control adenovirus did not have significant effects on TLR4, MyD88, and TRIF protein expression in LPS-induced ALI rats ($P > 0.05$ *vs.* LPS-treated and LPS + Ad.V-treated rats) (Fig. 9).

Downregulation of PALM3 Inhibits the Interaction of TLR4 with MyD88 or TRIF in Lung Tissue

MyD88 and TRIF are recruited to the TLR4 intracellular domain after stimulation by LPS, which triggers the formation of TLR4/MyD88 and TLR4/TRIF complexes [28]. As shown in Fig. 10, the formation of TLR4/MyD88 and TLR4/TRIF complexes was significantly increased in lung tissues after LPS stimulation ($P < 0.05$ *vs.* normal rats). Pre-treatment with Ad.PALM3-shRNA reduced the

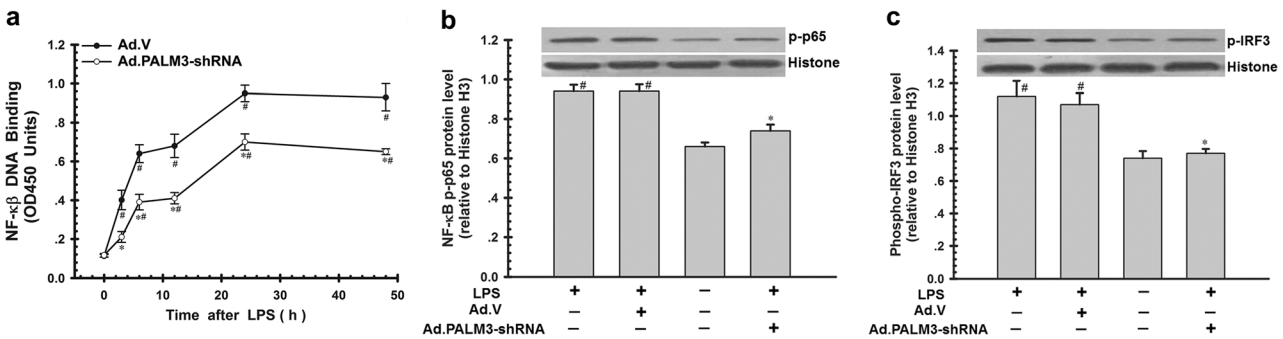

Fig. 8. Downregulation of PALM3 suppresses LPS-induced NF-κB and IRF3 activation in lungs. Rat lung tissues were collected and the NF-κB-DNA-binding activity (**a**) was measured by ELISA. Data are expressed as means ± SEM ($n = 6$). *$P < 0.05$ *vs.* Ad.V group at each time point and #$P < 0.05$ *vs.* 0 h time point. **b** Detection of NF-κB phosphor-p65 protein levels in lung tissues at 24 h after LPS-stimulation by western blot. Upper panel of **b** is a representative photograph. Normal and ALI rats were used as control groups. **c** Detection of the phospho-IRF-3 protein levels in lung tissues at 24 h after LPS-stimulation by western blot. Upper panel of **c** is a representative photograph. Normal and ALI rats were used as control groups. Data are expressed as means ± SEM ($n = 6$). *$P < 0.05$ *vs.* LPS-treated and LPS + Ad.V-treated rats and #$P < 0.05$ *vs.* normal rats.

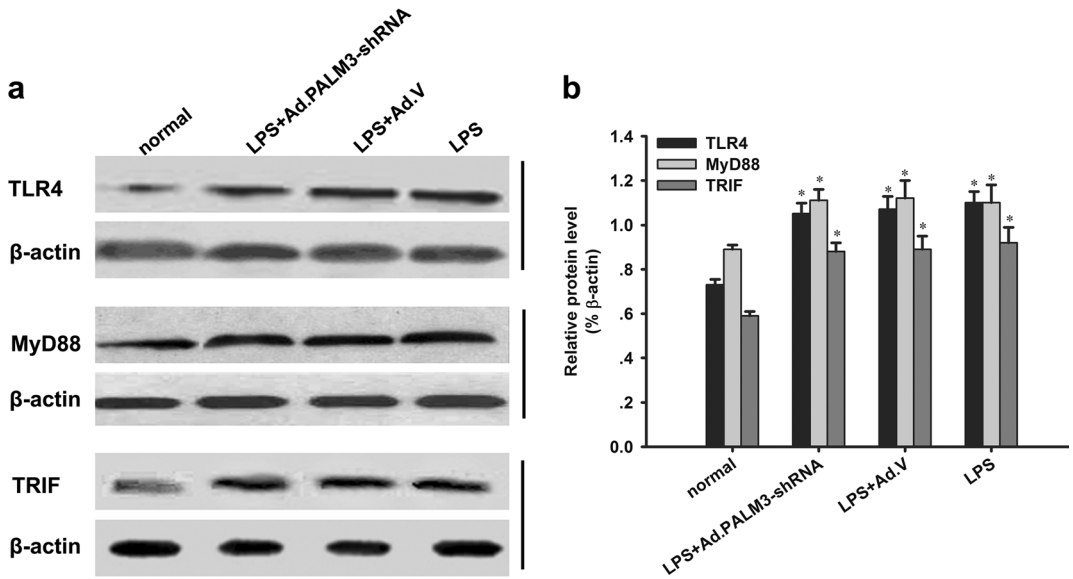

Fig. 9. The downregulation of PALM3 has no effect on LPS-induced TLR4, MyD88, and TRIF protein expression. Rats were instilled with 100 μL of Ad.PALM3-shRNA or Ad.V intranasally. At 48 h, lung injury was induced by a peritoneal injection of LPS (15 mg/kg). Normal and ALI rats were used as control groups, and lung tissues were collected at 24 h after LPS challenge. **a** Representative immunoblots of TLR4, MyD88, and TRIF. β-actin served as an internal control. **b** Quantification of densitometric measurement as a ratio of TLR4, MyD88, and TRIF relative to β-actin. Data are expressed as means ± SEM ($n = 6$). *$P < 0.05$ *vs.* normal rats.

intensity of the MyD88 and TRIF band coimmunoprecipitated using anti-TLR4 antibody ($P < 0.05$ *vs.* LPS-treated and LPS + Ad.V-treated rats). However, the control adenovirus (Ad.V) pre-treatment did not have significant effects on LPS-induced TLR4/MyD88 and TLR4/TRIF complex formation in comparison with LPS-treated rats ($P > 0.05$ *vs.* LPS-treated rats) (Fig. 10).

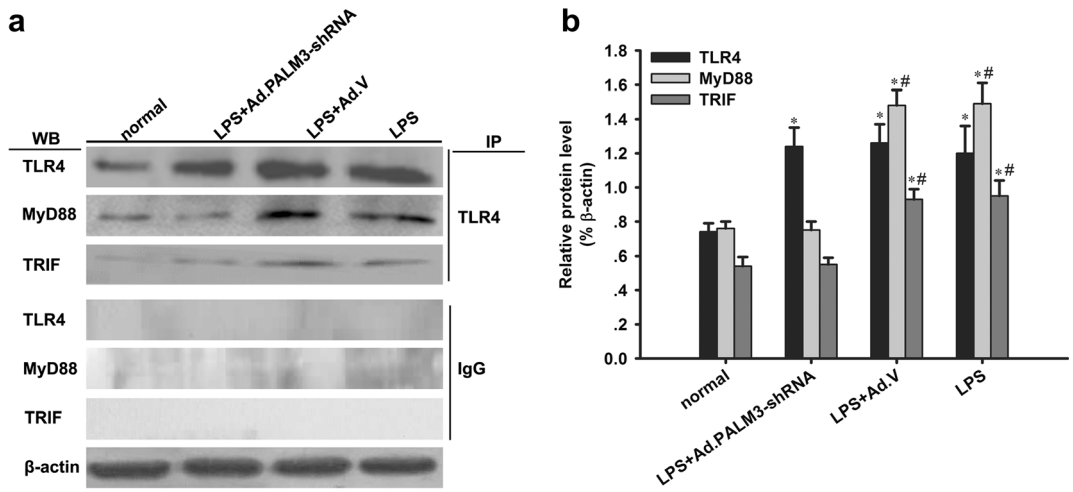

Fig. 10. Effects of downregulation of PALM3 on LPS-induced TLR4/MyD88 and TLR4/TRIF complex formation in lungs. Rats were instilled with 100 μL of Ad.PALM3-shRNA or Ad.V intranasally. At 48 h, lung injury was induced by a peritoneal injection of LPS (15 mg/kg). Normal and ALI rats were used as control groups, and lung tissues were collected at 24 h after LPS challenge. **a** Representative coimmunoprecipitated bands of MyD88 and TRIF by anti-TLR4 antibody. β-actin served as an internal control. **b** Quantification of densitometric measurement of PALM3 knockdown on interactions of TLR4 with MyD88 and TRIF. Data are expressed as means ± SEM ($n = 6$). *$P < 0.05$ *vs.* normal rats and #$P < 0.05$ *vs.* LPS + Ad.PALM3-shRNA-treated rats.

DISCUSSION

The present study revealed that PALM3 expression in rat lung was upregulated in a time-dependent manner in response to LPS. Furthermore, the downregulation of PALM3 improved the survival rate of rats, ameliorated the severity of lung injury, alleviated pulmonary edema, lung vascular leakage and neutrophil infiltration, inhibited the production of proinflammatory cytokines (TNF-α, IL-1β, and IFN-β) and activation of NF-κB and IRF3, and promoted the secretion of the anti-inflammatory cytokine IL-10 and the expression of SOCS3 in the LPS-induced ALI rat model. However, the downregulation of PALM3 did impact the upregulation of TLR4, MyD88, and TRIF protein expression induced by LPS in rat lung tissues. Moreover, the downregulation of PALM3 impeded the interaction of TLR4 with MyD88 or TRIF induced by LPS in rat lungs. These results suggest that the downregulation of PALM3 exerts a potential protective effect against LPS-induced ALI in rats and may be a promising potential treatment for ALI. Its protective effects were partially associated with the downregulation of proinflammatory cytokines, upregulation of the anti-inflammatory cytokine (IL-10) and negative regulator of inflammation (SOCS3), and the inhibition of NF-κB and IRF3 activities. Its mechanisms may be attributed to the modulation of inflammatory responses and inhibition of TLR4/MyD88 and TLR4/TRIF complex formation.

PALMs are a small protein family that includes PALM1, PALM2, PALM3, and palmdelphin (PALMD) [29], which are highly expressed in the brain, kidney, adrenal gland, mammary gland, and breast cancers [30–32]. Previous studies have verified that PALM1 is implicated in controlling cell shape, plasma membrane dynamics, cell motility, invasiveness and metastatic potential of cancer cells, modulation of cell migration and maturation, and tumor lymphangiogenesis [30, 31, 33]. However, little is known about the biological functions of the other PALM isoforms. Hultqvist and colleagues [34] considered that there is functional diversification and specific biological roles among PALM isoforms. PALM3 was first reported in 1992 by Cornish et al. [13] and was speculated to act as an adaptor to link intrinsic membrane proteins to each other, to the cytoskeleton, or to motor proteins [12, 29]. We reported for the first time in 2011 that PALM3 is a novel interactive partner of SIGIRR, and we also found that LPS upregulated the expression of PALM3 [12]. Our present study confirms the findings of our previous studies, which demonstrated the modulation of PALM3 expression in response to LPS [12, 14]. Our results revealed that PALM3 expression was detected in the lung tissue of normal rats, and that the control adenovirus Ad.V had no effect on PALM3 expression. After LPS stimulation, PALM3 protein and mRNA expression levels in the lungs of the Ad.V group were significantly upregulated in a time-dependent manner, which was in line with our previous result *in vitro* [12]. Moreover, the expression pattern of PALM3 was similar with those of the adaptors in TLR signaling, including MyD88 and TRIF [35–38]. The pattern of PALM3 upregulation might be related to its functional involvement in LPS-TLR4 signal transduction, similar to the adaptors [12]. In our present study, PALM3 gene and protein expression in lung tissues was downregulated by administering a recombinant adenovirus expressing shRNA for rat PALM3. Although PALM3 expression in the Ad.PALM3-shRNA group increased after LPS stimulation for 6 h, this expression level remained lower than that of the normal and Ad.V group rats during the experiment. This result demonstrated that the PALM3 gene transcript in lung tissue was silenced successfully using the interference adenoviral vector-mediated RNA through intranasal instillation. Increased PALM3 expression levels in the lungs of the Ad.PALM3-shRNA group may also be caused by enhanced PALM3 gene transcription during the process of inflammatory signal transduction.

An uncontrolled inflammatory response is one of the most crucial factors in the pathogenesis of ALI [3, 4]. During the early stage of ALI, inflammatory and immune responses involve a vast of array of mediators; therefore, inhibition of the inflammatory cascade response is critical for the treatment of this disorder [39]. Downregulation of PALM3 gene transcription to impede TLR signal transduction at the early stage may inhibit the excessive inflammatory responses and improve the outcome of inflammatory diseases, including ALI/ARDS. Thus, we determined the survival rate, lung histological changes, pulmonary edema, lung vascular leakage, neutrophil infiltration, and MPO activity in the lung to assess the effect of downregulation of PALM3 on LPS-induced ALI in rats. Our findings showed that the downregulation of PALM3 expression significantly improved the aforementioned assessment indexes, similar to previous studies [12, 14]. However, in these previous studies, the underlying mechanisms have not been explored. LPS induces the dimerization of TLR4, resulting in conformational changes of the TLR4 homodimer that induces the recruitment of adaptor proteins containing TIR domains. TIR domains of TLR4 recruit TIR domain-containing adaptor proteins, MyD88-adaptor-like (MAL) and MyD88 (MyD88-dependent pathway), or TRIF and Toll-IL-1 receptor-containing adapter molecule 2 (TICAM-2) (MyD88-independent pathway) [27]. Activation of the MyD88-dependent pathway induces the activation and translocation of transcription factors such as NF-κB and activator

protein-1 (AP-1) in the nucleus and induces the production of proinflammatory cytokines [27]. Activation of the MyD88-independent pathway leads to the activation and translocation of the transcription factor IRF3 in the nucleus to induce the production of type I interferon [27]. The MyD88-independent pathway also plays a key role in the late-phase activation of NF-κB [9]. In the present study, we found that the downregulation of PALM3 suppressed NF-κB-DNA-binding activity and decreased NF-κB phospho-p65 and phospho-IRF3 protein levels in the nucleus of ALI rat lung tissues. These findings suggested that the downregulation of PALM3 inhibited the activation of NF-κB and IRF3 in the ALI rat model. The increase of proinflammatory cytokines in the BALF are thought to be indices of local pulmonary inflammation in ALI [4, 20, 22], and the levels of inflammatory mediators in serum generally reflect the extent of systemic inflammatory response and the prognosis of inflammatory diseases [20, 22, 40, 41]. In our present study, a significantly increased survival rate was observed in the Ad.PALM3-shRNA group, accompanied with a decrease in inflammatory mediator levels in the BALF and serum. These results suggest that this therapy directed to the lung through intranasal instillation inhibited local inflammation in the lungs and suppressed systemic inflammation to improve the outcome of ALI. Mitigation of pulmonary inflammation and reduction of alveolar capillary permeability decreased the translocation of inflammatory mediators from lung tissues into the systemic circulation ameliorating severity of the systemic inflammatory response [42, 43]. The negative effect of the downregulated expression of PALM3 on the production of proinflammatory cytokines and the infiltration of neutrophils might be ascribed to its negative regulatory function on transcription factors NF-κB and IRF3. Alleviation of inflammatory responses can finally lead to the amelioration of lung tissue damage. Our results also revealed that the downregulation of PALM3 did not impact the upregulation of TLR4, MyD88, and TRIF protein expression after ALI in lung tissues. Previous studies have shown that PALMs are associated with lipid rafts and have been proposed to function as adaptors between membrane proteins or with the cortical cytoskeleton [30, 34]. With this in mind, we speculated that the inhibition of PALM3 expression to impair its function with adaptors in the LPS-TLR4 signaling pathway may be a potential mechanism for the downregulation of PALM3 protection against LPS-induced inflammatory responses and lung injury. Downregulating the PALM3 suppression of transcription factors NF-κB and IRF3 might not be mediated by inhibiting the expression of the adaptors TLR4, MyD88, and TRIF in LPS-induced inflammation. Therefore, we further investigated the effect of the downregulation of PALM3 on the interaction of TLR4 with MyD88 or TRIF in lung tissues of ALI rats. The result of coimmunoprecipitation analysis showed that PALM3 knockdown inhibited the interaction of TLR4 with MyD88 or TRIF. Our previous study demonstrated that PALM3 interacted with the TIR domain of SIGIRR [12]. Moreover, our *in vitro* study reveals that PALM3 interacts with MyD88, IRAK-1, TRAF-6, and TICAM-2, important adaptors in the TLR signaling pathway, in a ligand-dependent manner (accepted but unpublished data). Therefore, we presumed that PALM3 might act as a "bridge" to link TLR4 to the adaptor proteins (MyD88, IRAK-1, TRAF-6, and TIACM-2) in LPS-TLR4 signal transduction. Downregulation of PALM3 expression might diminish the bridging efficacy of PALM3 during LPS-TLR4 signal transduction, which might reduce further the interaction of TLR4 with MyD88 or TRIF. Inhibition of TLR4/MyD88 and TLR4/TRIF complex formation may be a potential mechanism of the suppression of NF-κB and IRF3 activation in LPS-induced inflammation. Further investigation is still needed to illuminate the detailed molecular mechanisms of the regulatory effect of PALM3 on LPS-TLR4 signaling.

IL-10 is a negative feedback regulatory molecule in the TLR4 signaling pathway that degrades the NF-κB p65 subunit and inactivates mitogen-activated protein kinase (MAPK) signaling [23]. In this study, we also found that LPS-induced IL-10 expression in the BALF and serum was significantly increased after PALM3 gene silencing. This finding suggests that PALM3 inhibits anti-inflammatory cytokine IL-10 secretion in LPS-induced ALI. However, the downregulation of PALM3 decreased the inhibitory effect of PALM3 on IL-10 secretion. Promotion of anti-inflammatory cytokine IL-10 secretion may also be a possible mechanism of downregulation of PALM3 protection against LPS-induced lung injury. The detailed mechanisms of PALM3 inhibition against LPS-induced IL-10 secretion warrant further research.

Previous studies have shown that SOCS proteins have pivotal roles in attenuating cytokine and TLR signaling in myeloid cells [24]. In mice deficient for SOCS3 in hematopoietic and endothelial cells, injection with granulocyte-colony stimulating factor (G-CSF) induced a pronounced inflammatory response involving enhanced neutrophilia and neutrophil infiltration of multiple tissues [44]. Furthermore, the exogenous delivery of SOCS3 significantly enhanced the survival of mice challenged with LPS-induced endotoxic shock [45]. In the present study, we demonstrated that the downregulation of PALM3 promoted the expression of SOCS3 in the lung tissues of ALI rats. It was reported that IL-10 induced SOCS3 expression to inhibit the expression of inflammatory cytokines in LPS-stimulated macrophages [23]. Thus, downregulating the PALM3 promotion of SOCS3 expression might be

indirectly mediated by enhancing the expression of IL-10 in LPS-induced inflammation. The detailed molecular mechanisms of the regulatory effect of PALM3 on SOCS3 expression require further investigation.

The LPS model of lung injury displays the key features of clinical ARDS, including inflammation, pulmonary edema, and mortality, and is still widely used to investigate the pathogenesis and treatment of ALI and ARDS [4, 17, 25, 39]. Therefore, in the present study, we used the LPS-induced ALI rat model to investigate the effect of the downregulation of PALM3 on ALI. The rat ALI model may be superior to the mouse ALI model based on the following reasons. First, the availability of the rat genome will be extremely useful, as opportunities for comprehensive physiologic studies of lung injury are better in rats than in mice [15, 46]. Second, rats have a larger blood volume in contrast to mice, which benefits the analysis of cytokine levels in serum, to further illustrate the relationship between the local and systemic inflammation and the mechanisms of ALI.

The PALM gene family is an early gene family that has been maintained throughout vertebrate evolution and may be important for the development and plasticity of complex nervous systems [34]. At present, there are no relevant literature reports on PALM3 knockouts; therefore, whether PALM3 knockout possesses potentially fatal consequences remains unclear. The effect of PALM3 knockout on the entire animal and the pathophysiological changes of ALI in PALM3 knockout animals will be investigated in future studies by constructing PALM3 gene knockout rat models. With respect to ALI/ARDS, transgene expression does not need to last a lifetime and a single administration of adenoviral vector could cover the critical period of ALI/ARDS [42]. We therefore chose an adenoviral vector as a transient gene transfer tool in our study. Our results showed that although PALM3 expression increased in the PALM3-knockdown group after LPS stimulation for 6 h, this expression level did not exceed that of normal rats at all time points. This finding indicates that the RNA interference activity of Ad.PALM3-shRNA lasted for the duration of the experiment. Moreover, in this study, we did not determine the effect of PALM3 on inflammatory cells and immune cells, such as dendritic cells and macrophages, as it was not clear whether PALM3 was expressed in these cells; however, this was not the main emphasis of the present study. Future research will focus on this emerging issue using *in vitro* experiments.

In summary, our results demonstrated that PALM3 expression was induced by LPS in a time-dependent manner, and that downregulation of PALM3 in the lung, *via* interfering adenoviral vector-mediated RNA, improved the survival rate in an LPS-induced rat model. This protective effect of PALM3-knockdown on ALI might be mediated by attenuating pulmonary pathological injury, alleviating alveolar capillary permeability, and decreasing neutrophil infiltration. Downregulation of proinflammatory cytokine secretion, upregulation of anti-inflammatory cytokine secretion and SOCS3 expression, and inhibition of NF-κB and IRF3 activities likely represent the mechanisms for the downregulation of PALM3 protection against LPS-induced inflammatory responses and lung tissue injury. Downregulating PALM3 suppression of LPS-TLR4 signaling might not be mediated by modulating the expression of TLR4, MyD88, and TRIF, but rather through inhibiting the interaction of TLR4 with MyD88 or TRIF. These results suggest that modulating PALM3 expression may be a promising potential treatment for ALI/ARDS. Future research will focus on the emerging issues from this study and on the detailed molecular mechanisms of the PALM3 regulation of LPS-TLR4 signaling.

ACKNOWLEDGEMENTS

The authors thank the National Natural Science Foundation of China (Chen, X.X., No. 81300050; Feng, J., No. 31300946) and the Innovative Cultivation Foundation of Navy General Hospital of the PLA (Chen, X.X., No. CXPY201417) for their great support in financing these researches.

COMPLIANCE WITH ETHICAL STANDARDS

Conflict of Interest. The authors declare that they have no conflict of interests.

Funding. This study was funded by the National Natural Science Foundation of China (Chen, X.X., No. 81300050; Feng, J., No. 31300946) and the Innovative Cultivation Foundation of Navy General Hospital of the PLA (Chen, X.X., No. CXPY201417).

REFERENCES

1. Tang, L., J. Bai, C.S. Chung, J. Lomas-Neira, Y. Chen, X. Huang, and A. Ayala. 2015. Programmed cell death receptor ligand 1 modulates the regulatory T cells' capacity to repress shock/sepsis-induced indirect acute lung injury by recruiting phosphatase SRC homology region 2 domain-containing phosphatase 1. *Shock* 43: 47–54.

2. Li-Mei, W., T. Jie, W. Shan-He, M. Dong-Mei, and Y. Peng-Jiu. 2016. Anti-inflammatory and Anti-oxidative Effects of Dexpanthenol on Lipopolysaccharide Induced Acute Lung Injury in Mice. *Inflammation*.
3. Kim, W.Y., and S.B. Hong. 2016. Sepsis and acute respiratory distress syndrome: Recent update. *Tuberculosis and Respiratory Diseases* 79: 53–57.
4. Chen, X., Y. Zhao, X. Wu, and G. Qian. 2011. Enhanced expression of single immunoglobulin IL-1 receptor-related molecule ameliorates LPS-induced acute lung injury in mice. *Shock* 35: 198–204.
5. Yi, C., S.R. Wang, S.Y. Zhang, S.J. Yu, C.X. Jiang, M.H. Zhi, and Y. Huang. 2006. Effects of recombinant human growth hormone on acute lung injury in endotoxemic rats. *Inflammation Research: Official Journal of the European Histamine Research Society ... [et al.]* 55: 491–497.
6. Lissauer, M.E., S.B. Johnson, G.V. Bochicchio, C.J. Feild, A.S. Cross, J.D. Hasday, C.C. Whiteford, W.A. Nussbaumer, M. Towns, and T.M. Scalea. 2009. Differential expression of toll-like receptor genes: sepsis compared with sterile inflammation 1 day before sepsis diagnosis. *Shock* 31: 238–244.
7. O'Neill, L.A., and C.A. Dinarello. 2000. The IL-1 receptor/toll-like receptor superfamily: crucial receptors for inflammation and host defense. *Immunology Today* 21: 206–209.
8. Sugiyama, K., M. Muroi, M. Kinoshita, O. Hamada, Y. Minai, Y. Sugita-Konishi, Y. Kamata, and K. Tanamoto. 2016. NF-κB activation via MyD88-dependent Toll-like receptor signaling is inhibited by trichothecene mycotoxin deoxynivalenol. *The Journal of Toxicological Sciences* 41: 273–279.
9. Shim, D.W., J.W. Han, X. Sun, C.H. Jang, S. Koppula, T.J. Kim, T.B. Kang, and K.H. Lee. 2013. Lysimachia clethroides Duby extract attenuates inflammatory response in Raw 264.7 macrophages stimulated with lipopolysaccharide and in acute lung injury mouse model. *Journal of Ethnopharmacology* 150: 1007–1015.
10. Wald, D., J. Qin, Z. Zhao, Y. Qian, M. Naramura, L. Tian, J. Towne, J.E. Sims, G.R. Stark, and X. Li. 2003. SIGIRR, a negative regulator of toll-like receptor-interleukin 1 receptor signaling. *Nature Immunology* 4: 920–927.
11. Xiao, H., M.F. Gulen, J. Qin, J. Yao, K. Bulek, D. Kish, C.Z. Altuntas, D. Wald, C. Ma, H. Zhou, V.K. Tuohy, R.L. Fairchild, C. de la Motte, D. Cua, B.A. Vallance, and X. Li. 2007. The Toll-interleukin-1 receptor member SIGIRR regulates colonic epithelial homeostasis, inflammation, and tumorigenesis. *Immunity* 26: 461–475.
12. Chen, X., X. Wu, Y. Zhao, G. Wang, J. Feng, Q. Li, and G. Qian. 2011. A novel binding protein of single immunoglobulin IL-1 receptor-related molecule: Paralemmin-3. *Biochemical and Biophysical Research Communications* 404: 1029–1033.
13. Cornish, J.A., M. Kloc, G.L. Decker, B.A. Reddy, and L.D. Etkin. 1992. Xlcaax-1 is localized to the basolateral membrane of kidney tubule and other polarized epithelia during Xenopus development. *Developmental Biology* 150: 108–120.
14. Li, S., L. Guo, Y. Zhao, P. Qian, X. Lv, L. Qian, Q. Wang, G. Qian, W. Yao, and X. Wu. 2016. Silencing of Paralemmin-3 Protects Mice from lipopolysaccharide-induced acute lung injury. *Peptides* 76: 65–72.
15. Matthay, M.A., G.A. Zimmerman, C. Esmon, J. Bhattacharya, B. Coller, C.M. Doerschuk, J. Floros, M.A. Gimbrone, E. Hoffman, R.D. Hubmayr, M. Leppert, S. Matalon, R. Munford, P. Parsons, A.S. Slutsky, K.J. Tracey, P. Ward, D.B. Gail, and A.L. Harabin. 2003. Future research directions in acute lung injury: summary of a National Heart, Lung, and Blood Institute working group. *American Journal of Respiratory and Critical Care Medicine* 167: 1027–1035.
16. Reynolds, P., P. Wall, M. van Griensven, K. McConnell, C. Lang, and T. Buchman. 2012. Shock supports the use of animal research reporting guidelines. *Shock* 38: 1–3.
17. Wang, Q., J. Wang, M. Hu, Y. Yang, L. Guo, J. Xu, C. Lei, Y. Jiao, and J. Xu. 2016. Uncoupling Protein 2 Increases Susceptibility to Lipopolysaccharide-Induced Acute Lung Injury in Mice. *Mediators of Inflammation* 2016: 9154230.
18. Wang, Y., M. Mao, and J.C. Xu. 2011. Cell-surface nucleolin is involved in lipopolysaccharide internalization and signalling in alveolar macrophages. *Cell Biology International* 35: 677–685.
19. Liu, W., M. Dong, L. Bo, C. Li, Q. Liu, Y. Li, L. Ma, Y. Xie, E. Fu, D. Mu, L. Pan, F. Jin, and Z. Li. 2014. Epigallocatechin-3-gallate ameliorates seawater aspiration-induced acute lung injury via regulating inflammatory cytokines and inhibiting JAK/STAT1 pathway in rats. *Mediators of Inflammation* 2014: 612593.
20. Xu, J., J. Qu, L. Cao, Y. Sai, C. Chen, L. He, and L. Yu. 2008. Mesenchymal stem cell-based angiopoietin-1 gene therapy for acute lung injury induced by lipopolysaccharide in mice. *The Journal of Pathology* 214: 472–481.
21. Huang, S.H., S. Duan, T. Sun, J. Wang, L. Zhao, Z. Geng, J. Yan, H.J. Sun, and Z.Y. Chen. 2011. JIP3 mediates TrkB axonal anterograde transport and enhances BDNF signaling by directly bridging TrkB with kinesin-1. *The Journal of Neuroscience: the Official Journal of the Society for Neuroscience* 31: 10602–10614.
22. Bai, J., L. Tang, J. Lomas-Neira, Y. Chen, K.R. McLeish, S.M. Uriarte, C.S. Chung, and A. Ayala. 2015. TAT-SNAP-23 treatment inhibits the priming of neutrophil functions contributing to shock and/or sepsis-induced extra-pulmonary acute lung injury. *Innate Immunity* 21: 42–54.
23. Liu, L.M., W.J. Tu, T. Zhu, X.T. Wang, Z.L. Tan, H. Zhong, D.Y. Gao, and D.Y. Liang. 2016. IRF3 is an important molecule in the UII/UT system and mediates immune inflammatory injury in acute liver failure. *Oncotarget*.
24. Wormald, S., and D.J. Hilton. 2007. The negative regulatory roles of suppressor of cytokine signaling proteins in myeloid signaling pathways. *Current Opinion in Hematology* 14: 9–15.
25. Zhao, J., H. Yu, Y. Liu, S.A. Gibson, Z. Yan, X. Xu, A. Gaggar, P.K. Li, C. Li, S. Wei, E.N. Benveniste, and H. Qin. 2016. Protective effect of suppressing STAT3 activity in LPS-induced acute lung injury. *American Journal of Physiology. Lung Cellular and Molecular Physiology* 311: L868–868L880.
26. Wu, Q., R. Li, L.W. Soromou, N. Chen, X. Yuan, G. Sun, B. Li, and H. Feng. 2014. p-Synephrine suppresses lipopolysaccharide-induced acute lung injury by inhibition of the NF-κB signaling pathway. *Inflammation Research : Official Journal of the European Histamine Research Society ... [et al.]* 63: 429–439.
27. Molteni, M., S. Gemma, and C. Rossetti. 2016. The Role of Toll-Like Receptor 4 in Infectious and Noninfectious Inflammation. *Mediators of Inflammation* 2016: 6978936.
28. Ding, Y., H. Yang, W. Xiang, X. He, W. Liao, and Z. Yi. 2015. CD200R1 agonist attenuates LPS-induced inflammatory response in human renal proximal tubular epithelial cells by regulating TLR4-MyD88-TAK1-mediated NF-κB and MAPK pathway. *Biochemical and Biophysical Research Communications* 460: 287–294.
29. Hu, B., E. Petrasch-Parwez, M.M. Laue, and M.W. Kilimann. 2005. Molecular characterization and immunohistochemical localization of palmdelphin, a cytosolic isoform of the paralemmin protein family implicated in membrane dynamics. *European Journal of Cell Biology* 84: 853–866.
30. Kutzleb, C., G. Sanders, R. Yamamoto, X. Wang, B. Lichte, E. Petrasch-Parwez, and M.W. Kilimann. 1998. Paralemmin, a prenyl-palmitoyl-anchored phosphoprotein abundant in neurons

and implicated in plasma membrane dynamics and cell process formation. *The Journal of Cell Biology* 143: 795–813.

31. Albrecht, I., R. Bieri, A. Leu, P. Granacher, J. Hagmann, M.W. Kilimann, and G. Christofori. 2013. Paralemmin-1 is expressed in lymphatic endothelial cells and modulates cell migration, cell maturation and tumor lymphangiogenesis. *Angiogenesis* 16: 795–807.
32. Turk, C.M., K.D. Fagan-Solis, K.E. Williams, J.M. Gozgit, S. Smith-Schneider, S.A. Marconi, C.N. Otis, G.M. Crisi, D.L. Anderton, M.W. Kilimann, and K.F. Arcaro. 2012. Paralemmin-1 is over-expressed in estrogen-receptor positive breast cancers. *Cancer Cell International* 12: 17.
33. Kutzleb, C., E. Petrasch-Parwez, and M.W. Kilimann. 2007. Cellular and subcellular localization of paralemmin-1, a protein involved in cell shape control, in the rat brain, adrenal gland and kidney. *Histochemistry and Cell Biology* 127: 13–30.
34. Hultqvist, G., D.D. Ocampo, D. Larhammar, and M.W. Kilimann. 2012. Evolution of the vertebrate paralemmin gene family: ancient origin of gene duplicates suggests distinct functions. *PloS One* 7: e41850.
35. He, Z., Y. Zhu, and H. Jiang. 2009. Inhibiting toll-like receptor 4 signaling ameliorates pulmonary fibrosis during acute lung injury induced by lipopolysaccharide: An experimental study. *Respiratory Research* 10: 126.
36. Van Linthout, S., F. Spillmann, G. Graiani, K. Miteva, J. Peng, E. Van Craeyveld, M. Meloni, M. Tölle, F. Escher, A. Subasigüller, W. Doehner, F. Quaini, B. De Geest, H.P. Schultheiss, and C. Tschöpe. 2011. Down-regulation of endothelial TLR4 signalling after apo A-I gene transfer contributes to improved survival in an experimental model of lipopolysaccharide-induced inflammation. *Journal of Molecular Medicine: Official Organ of the "Gesellschaft Deutscher Naturforscher und Ärzte"* 89: 151–160.
37. Li, S., H. Lu, X. Hu, W. Chen, Y. Xu, and J. Wang. 2010. Expression of TLR4-MyD88 and NF-κB in the iris during endotoxin-induced uveitis. *Mediators of Inflammation* 2010: 748218.
38. Shan, Y., N. Lin, X. Yang, J. Tan, R. Zhao, S. Dong, and S. Wang. 2012. Sulphoraphane inhibited the expressions of intercellular adhesion molecule-1 and vascular cell adhesion molecule-1 through MyD88-dependent toll-like receptor-4 pathway in cultured endothelial cells. *Nutrition, Metabolism, and Cardiovascular Diseases: NMCD* 22: 215–222.
39. Liu, Y.L., Y.J. Liu, Y. Liu, X.S. Li, S.H. Liu, Y.G. Pan, J. Zhang, Q. Liu, and Y.Y. Hao. 2014. Hydroxysafflor yellow A ameliorates lipopolysaccharide-induced acute lung injury in mice via modulating toll-like receptor 4 signaling pathways. *International Immunopharmacology* 23: 649–657.
40. Guo, L., S. Li, Y. Zhao, P. Qian, F. Ji, L. Qian, X. Wu, and G. Qian. 2015. Silencing Angiopoietin-Like Protein 4 (ANGPTL4) Protects Against Lipopolysaccharide-Induced Acute Lung Injury Via Regulating SIRT1 /NF-kB Pathway. *Journal of Cellular Physiology* 230: 2390–2402.
41. Zhao, Y.F., W. Xiong, and X.L. Wu. 2014. Mesenchymal stem cell-based developmental endothelial locus-1 gene therapy for acute lung injury induced by lipopolysaccharide in mice. *Molecular Medicine Reports* 9: 1583–1589.
42. Baba, Y., T. Yazawa, Y. Kanegae, S. Sakamoto, I. Saito, N. Morimura, T. Goto, Y. Yamada, and K. Kurahashi. 2007. Keratinocyte growth factor gene transduction ameliorates acute lung injury and mortality in mice. *Human Gene Therapy* 18: 130–141.
43. Panos, R.J., P.M. Bak, W.S. Simonet, J.S. Rubin, and L.J. Smith. 1995. Intratracheal instillation of keratinocyte growth factor decreases hyperoxia-induced mortality in rats. *The Journal of Clinical Investigation* 96: 2026–2033.
44. Croker, B.A., D. Metcalf, L. Robb, W. Wei, S. Mifsud, L. DiRago, L.A. Cluse, K.D. Sutherland, L. Hartley, E. Williams, J.G. Zhang, D.J. Hilton, N.A. Nicola, W.S. Alexander, and A.W. Roberts. 2004. SOCS3 is a critical physiological negative regulator of G-CSF signaling and emergency granulopoiesis. *Immunity* 20: 153–165.
45. Fang, M., H. Dai, G. Yu, and F. Gong. 2005. Gene delivery of SOCS3 protects mice from lethal endotoxic shock. *Cellular & Molecular Immunology* 2: 373–377.
46. Jacob, H.J., and A.E. Kwitek. 2002. Rat genetics: attaching physiology and pharmacology to the genome. *Nature Reviews. Genetics* 3: 33–42.